

## ORIGINAL RESEARCH—BASIC

Paneth Cell Secretion *in vivo* Requires Expression of Tmem16a and Tmem16fRainer Schreiber,<sup>1</sup> Ines Cabrita,<sup>2</sup> and Karl Kunzelmann<sup>1</sup><sup>1</sup>Institut für Physiologie, Universität Regensburg, Regensburg, Bavaria, Germany; and <sup>2</sup>Nephrologisches Forschungslabor, University of Cologne, Köln, NRW, Germany

**BACKGROUND AND AIMS:** Paneth cells play a central role in intestinal innate immune response. These cells are localized at the base of small intestinal crypts of Lieberkuhn. The calcium-activated chloride channel TMEM16A and the phospholipid scramblase TMEM16F control intracellular  $Ca^{2+}$  signaling and exocytosis. We analyzed the role of TMEM16A and TMEM16F for Paneth cells secretion. **METHODS:** Mice with intestinal epithelial knockout of Tmem16a (Tmem16a<sup>-/-</sup>) and Tmem16f (Tmem16f<sup>-/-</sup>) were generated. Tissue structures and Paneth cells were analyzed, and Paneth cell exocytosis was examined in small intestinal organoids *in vitro*. Intracellular  $Ca^{2+}$  signals were measured and were compared between wild-type and Tmem16 knockout mice. Bacterial colonization and intestinal apoptosis were analyzed. **RESULTS:** Paneth cells in the crypts of Lieberkuhn from Tmem16a<sup>-/-</sup> and Tmem16f<sup>-/-</sup> mice demonstrated accumulation of lysozyme. Tmem16a and Tmem16f were localized in wild-type Paneth cells but were absent in cells from knockout animals. Paneth cell number and size were enhanced in the crypt base and mucus accumulated in intestinal goblet cells of knockout animals. Granule fusion and exocytosis on cholinergic and purinergic stimulation were examined online. Both were strongly compromised in the absence of Tmem16a or Tmem16f and were also blocked by inhibition of Tmem16a/f. Purinergic  $Ca^{2+}$  signaling was largely inhibited in Tmem16a knockout mice. Jejunal bacterial content was enhanced in knockout mice, whereas cellular apoptosis was inhibited. **CONCLUSION:** The present data demonstrate the role of Tmem16 for exocytosis in Paneth cells. Inhibition or activation of Tmem16a/f is likely to affect microbial content and immune functions present in the small intestine.

**Keywords:** Paneth Cells; Exocytosis; TMEM16A; Anoctamin 1; ANO1; TMEM16F; Anoctamin 6; ANO6; Goblet Cells; Secretion;  $Ca^{2+}$ -Activated  $Cl^-$  Channel; Phospholipid Scrambling

## Introduction

Paneth cells have a central function in intestinal innate immune response.<sup>1–3</sup> Paneth cells are located in the base of small intestinal crypts of Lieberkuhn and have defensive functions that include protection of stem cells in response to invading microbes and eradication of ingested pathogens. Together with other secretory cells, they clear pathogens from intestinal crypts.<sup>4</sup> By means of secreted

factors, they also regulate the composition and number of commensal intestinal bacteria.<sup>5</sup> Paneth cells are filled with rather large granules that contain antimicrobial proteins/peptides, such as lysozyme, secretory phospholipase-A2, and defensins, and they also secrete cytokines to recruit immune cells.<sup>6</sup> During Paneth cell metaplasia in inflammatory bowel disease or as a response to mucosal damage, the Paneth cell zone expands due to increase in cell size and cell number.<sup>7</sup>

It was shown that cholinergic stimulation confers enhanced protection in animals orally infected with virulent *Salmonella enterica*.<sup>8</sup> Acetylcholine binds to basolateral M3 muscarinic receptors allowing adaptive immunity to helminth and bacterial infection.<sup>9</sup> However, the mechanisms of luminal stimulation of Paneth cell secretion via live bacteria or lipopolysaccharide (LPS) are unclear.<sup>4</sup> Paneth cells do not express Toll-like receptor 4 (TLR4), the receptor for LPS.<sup>10–12</sup> However, LPS can also trigger immune response independent of TLR4 by binding to LPS-binding protein, which is then internalized by the host cell.<sup>13,14</sup> It was shown that uptake of LPB/LPS triggers subsequent adenosine triphosphate (ATP) release.<sup>15</sup>

We recently reported for the first-time activation of intestinal mucus secretion by luminal and basolateral ATP.<sup>16</sup> ATP activates mucus secretion via activation of purinergic P2Y2 receptors and release of  $Ca^{2+}$  to the apical sub-membraneous compartment. For efficient release of  $Ca^{2+}$  via inositol trisphosphate (IP3)-activated  $Ca^{2+}$  release channels (IP3R) located in the endoplasmic reticulum (ER), IP3R is tethered to the apical compartment by binding to the  $Ca^{2+}$ -activated  $Cl^-$  channel TMEM16A (anoctamin 1, ANO1).<sup>16,17</sup> High local  $Ca^{2+}$  levels in the apical intracellular compartment support the exocytic machinery in intestinal and airway goblet cells.<sup>18,19</sup> Importantly, ATP-induced

**Abbreviations used in this paper:** ATP, adenosine triphosphate; CCH, carbachol; CF, cystic fibrosis; ER, endoplasmic reticulum; LPS, lipopolysaccharide; TLR4, Toll-like receptor 4; TUNEL, Terminal deoxynucleotidyl transferase dUTP nick end labeling; WT, wild type.

Most current article

Copyright © 2022 Published by Elsevier Inc. on behalf of the AGA Institute. This is an open access article under the CC BY-NC-ND license (<http://creativecommons.org/licenses/by-nc-nd/4.0/>).

2772-5723

<https://doi.org/10.1016/j.gastha.2022.08.002>

mucus secretion by secretory cells was compromised in both intestine and airways of Tmem16a knockout mice (Tmem16a<sup>-/-</sup>).<sup>18</sup> As a consequence, mucus accumulated in intestinal and airway goblet cells of Tmem16a<sup>-/-</sup> mice. A similar but less pronounced mucus accumulation was also observed in Tmem16f<sup>-/-</sup> mice.<sup>20</sup> Here, we demonstrate the role of Tmem16a and Tmem16f for exocytosis in Paneth cells and describe the underlying molecular mechanisms. The present findings are of clinical relevance, because many small molecules and natural or herbal compounds exist that either activate or inhibit both Tmem16a and Tmem16f.<sup>21,22</sup>

## Methods

### Animals

Generation of mice with intestinal epithelial-specific knockout of Tmem16a (Tmem16a<sup>-/-</sup>) or Tmem16f (Tmem16f<sup>-/-</sup>) and genotyping has been reported earlier.<sup>20,23</sup>

### Intestinal Crypts Isolation, Organoids Culture, and Life Microscopy Imaging (Differential Interference Contrast)

Isolation of intestinal crypts and culturing of organoids were done as described by Mahe et al.<sup>24</sup> and Altay et al.<sup>25</sup> Organoids in Matrigel (Corning, Wiesbaden, Germany) were cultured on glass coverslips in media containing (GIBCO; Thermo Fisher, Scientific, Waltham, MA, USA) Advanced DMEM/F-12, L-glutamine, (4-(2-hydroxyethyl)-1-piperazineethanesulfonic acid), penicillin/streptomycin, N2 supplement, B27 supplement, mouse recombinant EGF (Sigma-Aldrich, Merck KGaA, Darmstadt, Germany), Mouse Recombinant Noggin (PeproTech, Hamburg, Germany), Human Recombinant R-Spondin-1 (PeproTech), and N-acetyl-L-cysteine (Sigma-Aldrich, Merck KGaA). Three- to six-day-old organoids were mounted into a chamber overlaid with 100  $\mu$ L Ringer solution (NaCl 145 mmol/L; KH<sub>2</sub>PO<sub>4</sub> 0.4 mmol/L; K<sub>2</sub>HPO<sub>4</sub> 1.6 mmol/L; glucose 5 mmol/L; MgCl<sub>2</sub> 1 mmol/L; Ca<sup>2+</sup>-Gluconate 1.3 mmol/L). Paneth cells were observed under an Axiovert Observer microscope (Carl Zeiss Microscopy Deutschland GmbH, Oberkochen, Germany) using differential interference contrast. Pictures are taken every 10 seconds using the ZEN software (Carl Zeiss Microscopy Deutschland GmbH). Secretion was stimulated by ATP (100  $\mu$ M; Sigma-Aldrich, Merck KGaA) and subsequently with carbachol (CCH, 10  $\mu$ M; Sigma-Aldrich, Merck KGaA). Granule secretion was analyzed according to Yokoi et al.<sup>4</sup> using the ZEN software.

### Histology and Immunohistochemistry of Tmem16a, Tmem16f, and Lysozyme

Mouse duodenum, jejunum, and ileum were fixed with 4% paraformaldehyde, 0.2% picric acid, and 3.4% sucrose overnight, dehydrated, and embedded in paraffin. The paraffin-embedded tissues were cut at 4  $\mu$ m on a rotary microtome (Leica Mikrotom RM 2165, Wetzlar, Germany). The sections were dewaxed and rehydrated. For histology or mucus analysis, sections were stained according to standard hematoxylin/eosin or periodic acid-Schiff protocols and examined by light microscopy. For

immunohistochemistry, sections were cooked in Tris/ethylenediaminetetraacetic acid (pH8.5, TMEM16A or TMEM16F staining) or citrate buffer (pH 6, for lysozyme staining) for 15 minutes and permeabilized and blocked with 0.04% Triton X-100 and 5% bovine serum albumin for 30 minutes at 37 °C. Sections were incubated with primary antibodies against mouse TMEM16A antigen MEECAPGGCLMELCIQL (Davids Biotechnologie GmbH, Regensburg, Germany), mouse TMEM16F antigen KRE-KYLTQKLLHESHLKDLTK (Davids Biotechnologie GmbH) or lysozyme (PA5\_16668; Invitrogen, Thermo Fisher, Scientific) in 0.5% bovine serum albumin and 0.04% Triton X-100 overnight at 4 °C and subsequent with a secondary goat anti-rabbit Alexa 488 or goat anti-rabbit Alexa 546 IgG (Invitrogen, Thermo Fisher, Scientific) for 1 hour at 37 °C. Sections were counterstained with Hoe33342 (Sigma-Aldrich, Merck KGaA). Immunofluorescence was detected using an Axiovert Observer microscope equipped with ApoTome2 and ZEN software.

### Apoptotic Cell Death in Mouse Intestine

Terminal deoxynucleotidyl transferase dUTP nick end labeling (TUNEL) was performed in 4% paraformaldehyde, 0.2% picric acid, and 3.4% sucrose fixed and in paraffin-embedded murine jejunum and ileum. For TUNEL assay, the DeadEnd Colorimetric TUNEL System (Promega, Mannheim, Germany) was used according to manufacturer's instructions and analyzed with ImageJ (NIH, USA).<sup>26</sup>

### Detection of Bacteria in Mouse Jejunum and Ileum

Gram-positive and Gram-negative bacteria were detected using Gram Stain Kit (Abcam, Amsterdam, the Netherlands). Briefly, after deparaffination and hydration, paraffin-embedded jejunum or ileum was incubated in Gientian violet solution and rinsed in water. Slides were incubated in Lugol's iodine solution and rinsed with water. Slides were decolorized with Gram decolorizer and then incubated in carbol fuchsin. After washing, the tissue elements were counterstained with tartrazine solution. The number of bacteria in cross-sections was analyzed using ImageJ.<sup>26</sup>

### Measurement of Intracellular Ca<sup>2+</sup> in Paneth Cells

Intestinal organoids on glass coverslips were loaded with 2  $\mu$ M Fura-2/AM and 0.02% Pluronic F-127 (Invitrogen, Thermo Fisher, Scientific) in ringer solution (NaCl 145 mmol/L; KH<sub>2</sub>PO<sub>4</sub> 0.4 mmol/L; K<sub>2</sub>HPO<sub>4</sub> 1.6 mmol/L; glucose 5 mmol/L; MgCl<sub>2</sub> 1 mmol/L; Ca<sup>2+</sup>-Gluconate 1.3 mmol/L) for 1 hour at room temperature. The agonists ATP and CCH were applied subsequently to increase intracellular Ca<sup>2+</sup> concentrations. Ca<sup>2+</sup> increase by application of CCH and ATP in reverse sequence was not significantly different. Fluorescence was detected at 37 °C using an inverted microscope (Axiovert S100, Carl Zeiss Microscopy Deutschland GmbH) and a high-speed polychromator system (VisiChrome, Puchheim, Germany). Fura-2 was excited at 340/380 nm, and emission was recorded between 470 nm and 550 nm using a CoolSnap camera (CoolSnap HQ, Visitron, Puchheim, Germany). [Ca<sup>2+</sup>]<sub>i</sub> was calculated from the 340/380 nm fluorescence ratio after background subtraction. The formula used to calculate [Ca<sup>2+</sup>]<sub>i</sub> was [Ca<sup>2+</sup>]<sub>i</sub> = Kd × (R - R<sub>min</sub>) / (R<sub>max</sub> - R) × (Sf2/Sb2), where R is the observed fluorescence ratio. The values R<sub>max</sub> and R<sub>min</sub> (maximum and minimum

ratios) and the constant Sf2/Sb2 (fluorescence of free and  $\text{Ca}^{2+}$ -bound Fura-2 at 380 nm) were calculated using  $1 \mu\text{M}$  ionomycin (Calbiochem, Merck KGaA, Darmstadt, Germany),  $5 \mu\text{M}$  nigericin,  $10 \mu\text{M}$  monensin (Sigma-Aldrich, Merck KGaA), and  $5 \text{ mM}$  EGTA to equilibrate intracellular and extracellular  $\text{Ca}^{2+}$  in intact Fura-2-loaded Paneth cells. The dissociation constant for the Fura-2· $\text{Ca}^{2+}$  complex was taken as  $224 \text{ nmol/L}$ . Control of experiments, imaging acquisition, and data analysis were done with the software package Meta-Fluor (Molecular Devices, Biberach, Germany).

### Materials and Statistical Analysis

All compounds used were of highest available grade of purity and were bought from Sigma-Aldrich (Merck KGaA, Darmstadt, Germany), unless indicated otherwise. Data are shown as individual traces/representative images and/or as summaries with mean values  $\pm$  standard error of the mean, with the respective number of experiments given in each figure legend. For statistical analysis, paired or unpaired Student's *t*-test, analysis of variance (post hoc Bonferroni), or Kruskal-Wallis test (H-Test) were used as appropriate. A *P*-value of  $< .05$  was accepted as a statistically significant difference.

## Results

### Accumulation of Lysozyme in Paneth Cells of Mice Lacking Expression of Tmem16a or Tmem16f

In previous studies, we detected the expression of Tmem16a and Tmem16f in mouse intestinal epithelial

cells.<sup>18,20,23,27</sup> Here, we analyzed the expression of Tmem16a and Tmem16f in the jejunal crypt base of wild-type (WT),  $\text{TMEM16a}^{-/-}$ , and  $\text{Tmem16f}^{-/-}$  mice. Tmem16a was detected at the apical pole, whereas expression of Tmem16f was located predominantly at the basolateral side of crypt epithelial cells (Figure 1A, Figure A1). Notably, Tmem16a is also located in intestinal smooth muscle cells. We detected a pronounced accumulation of lysozyme in jejunal Paneth cells of  $\text{TMEM16a}^{-/-}$  and  $\text{Tmem16f}^{-/-}$  mice when compared with WT animals (Figure 1B and C). These results suggested a Paneth cells secretory defect in the absence of TMEM16a or Tmem16f. Paneth cells at the crypt base can be easily identified by their abundant eosinophilic granules. When analyzing small intestinal Paneth cells, we detected an enhanced size of Paneth cells in  $\text{Tmem16f}^{-/-}$  mice (Figure 2A and B). Moreover, the number of Paneth cells per crypt and the number of granules within each Paneth cell were enhanced in  $\text{TMEM16a}^{-/-}$  and  $\text{Tmem16f}^{-/-}$  mice when compared with WT (Figure 2A and C).

### Accumulation of Intestinal Mucus in $\text{Tmem16a}^{-/-}$ and $\text{Tmem16f}^{-/-}$ Mice

Previous studies demonstrated airway goblet cell metaplasia, an accumulation of mucus in airway and intestinal goblet cells of mice with tissue-specific knockout of Tmem16a and Tmem16f.<sup>18,20,23</sup> A more detailed analysis of mucus using periodic acid-Schiff staining of duodenum,

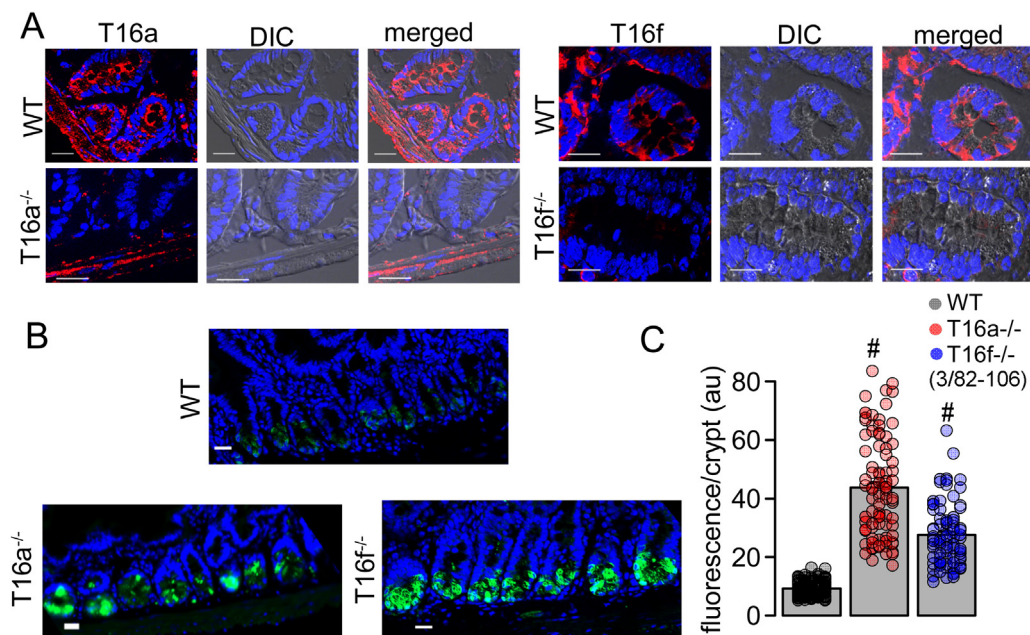


**Figure 1.** Loss of Tmem16a and Tmem16f cause defective lysozyme secretion by Paneth cells. (A) Expression of Tmem16a and Tmem16f in WT mice and knockout of  $\text{TMEM16a}^{-/-}$  and  $\text{Tmem16f}^{-/-}$  mice in jejunal crypts. Tmem16a is located in the apical pole, whereas the expression of Tmem16f is more located to the basolateral pole of crypt epithelial cells. (B) Staining of lysozyme in jejunal Paneth cells of wt mice (WT) and mice lacking expression of Tmem16a ( $\text{T16a}^{-/-}$ ) or Tmem16f ( $\text{T16f}^{-/-}$ ). (C) Fluorescence intensity measured per crypt demonstrates a pronounced accumulation of lysozyme in jejunal Paneth cells of  $\text{Tmem16a}^{-/-}$  and  $\text{Tmem16f}^{-/-}$  knockout mice. Bar indicates  $20 \mu\text{m}$ . Mean  $\pm$  standard error of the mean (number of animals and crypts analyzed). #significant difference from WT ( $P < .05$ , analysis of variance). WT, wild type.

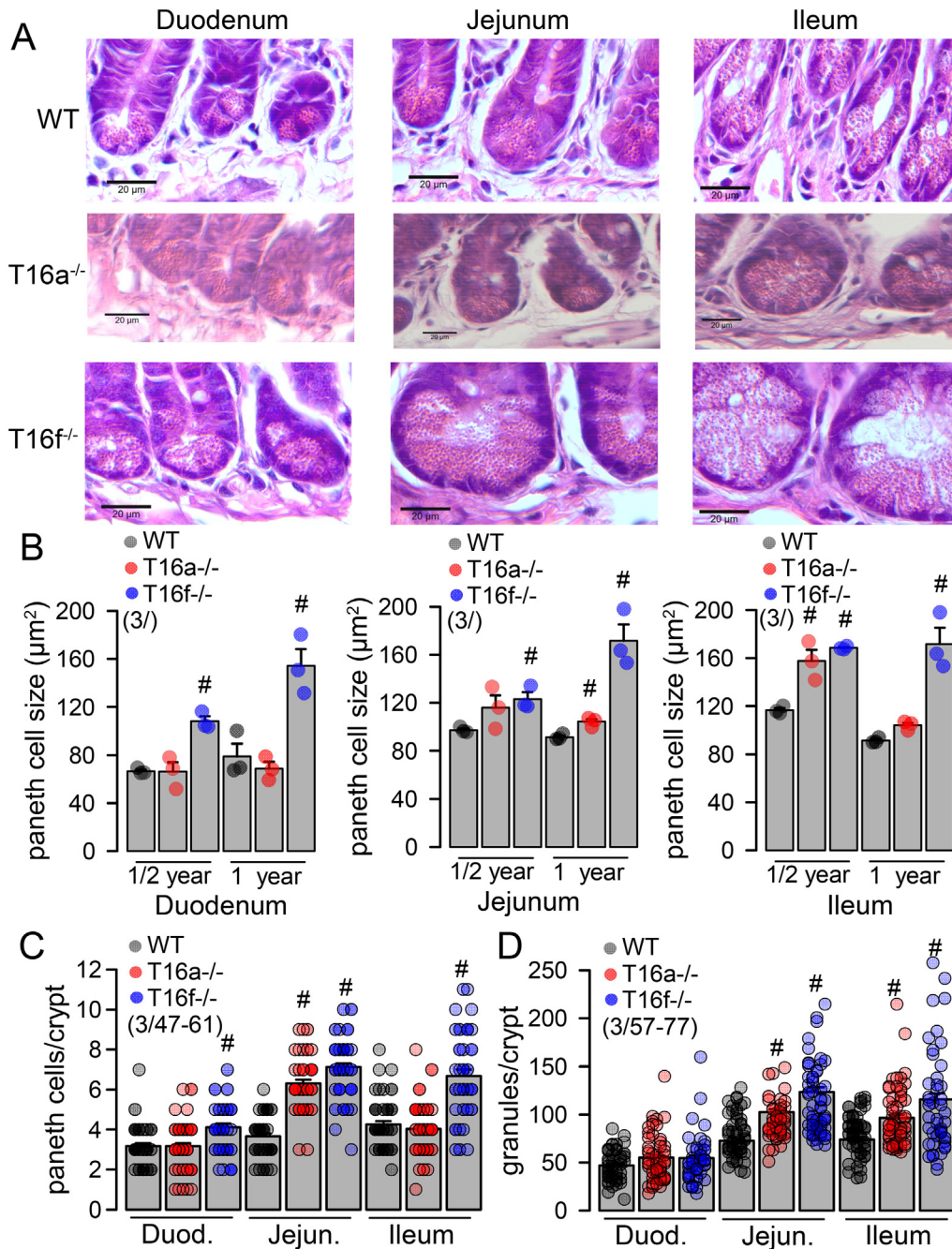


**Figure 2.** Number and size of Paneth cells are enhanced in *Tmem16a*<sup>-/-</sup> and *Tmem16f*<sup>-/-</sup> mice. (A) HE staining of crypt bases of duodenum, jejunum, and ileum of WT, *T16a*<sup>-/-</sup>, and *T16f*<sup>-/-</sup> mice. Bar = 20 µm. (B) Quantitative analysis of Paneth cell sizes in duodenum, jejunum, and ileum. (C, D) Analysis of Paneth cell number and number of granules within Paneth cells in duodenum, jejunum, and ileum of WT, *T16a*<sup>-/-</sup>, and *T16f*<sup>-/-</sup> mice. Mean ± standard error of the mean (number of animals and crypts analyzed). #significant difference from WT ( $P < .05$ , analysis of variance). WT, wild type.

jejunum, and ileum performed in the present study confirmed previous results and demonstrated enhanced mucus in small intestine of *TMEM16a*<sup>-/-</sup> and *Tmem16f*<sup>-/-</sup> mice (Figure 3, Figure A2). The data suggest that lack of either *Tmem16a* or *Tmem16f* causes a broad secretory defect in secretory cells, including Paneth cells.

### *ATP-Induced but not CCH-Induced Release of Granules From Paneth Cells is Compromised by Knockout of Tmem16a*

Accumulation of lysozyme in the knockout animals prompted us to examine in more detail the potential secretory defect in Paneth cells. To that end, we generated

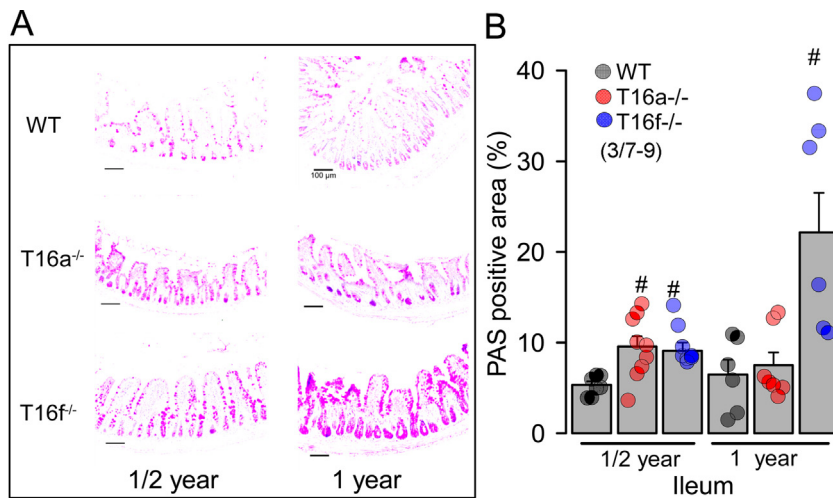


**Figure 3.** Accumulation of intestinal mucus in *Tmem16a<sup>-/-</sup>* and *Tmem16f<sup>-/-</sup>* mice. (A) PAS staining of ileum from WT, *T16a<sup>-/-</sup>*, and *T16f<sup>-/-</sup>* mice. Mucus staining was analyzed in 1/2-year-old and 1-year-old mice. Bar = 100 μm. (B) Quantitative analysis of PAS positivity in ileum of WT, *T16a<sup>-/-</sup>*, and *T16f<sup>-/-</sup>* mice. Mean ± standard error of the mean (number of animals and crypts analyzed). #significant difference from WT ( $P < .05$ , ANOVA). WT, wild type.

jejunal organoids by growing freshly isolated jejunal crypts in a three-dimensional matrigel. These organoids demonstrate features of naïve crypts with enterocytes, goblet cells, and lysozyme-expressing Paneth cells (Figure 4A). Granule-filled Paneth cells could be easily detected by life differential interference contrast microscopy (Figure 4B). In online experiments, organoids were exposed to the secretagogue CCH and to the purinergic ligand ATP. In WT organoids, CCH

induced a sudden and complete release of granules from Paneth cells (Figure 4B, WT\_CCH.mp4). In contrast, stimulation with ATP induced a slower and only partial release of granules in the apical compartment of Paneth cells (Figure 4B, WT\_ATP.mp4). Notably, apical application of ATP by injection into the lumen of organoids caused a similar apical release of granules (WT\_ATP\_apical injection.mp4). ATP-induced Paneth cell secretion was

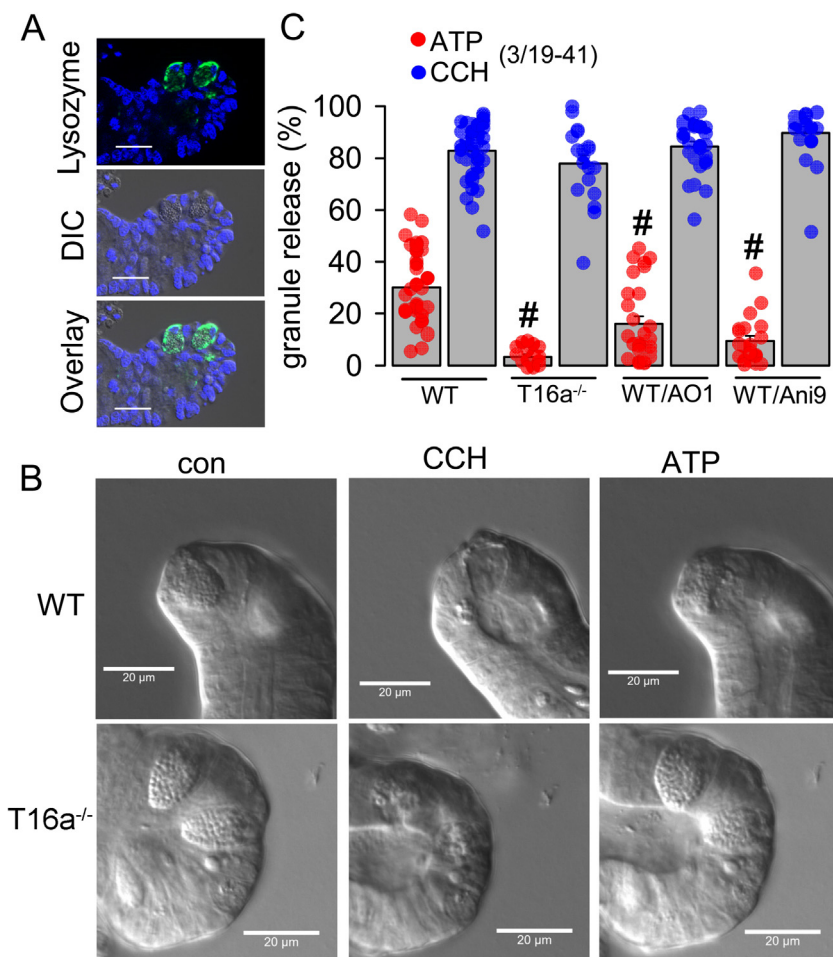


**Figure 4.** ATP-induced but not CCH-induced release of granules from Paneth cells is compromised by knockout of *Tmem16a*. (A) Lysozyme filled granules in Paneth cells present in jejunal organoids. (B) ATP (100 μM) and CCH (10 μM) induced release of granules from Paneth cells in jejunal organoids obtained from WT and *T16a<sup>-/-</sup>* mice. (C) Percent of granules being release from jejunal organoids upon stimulation with ATP or CCH (10 μM). Release of granules was assessed in WT and *T16a<sup>-/-</sup>* organoids and in WT organoids in the presence of the *Tmem16a*-blockers AO1 (10 μM) or Ani9 (10 μM). Bars = 20 μm. Mean ± standard error of the mean (number of animals and cells analyzed). #significant difference from WT ( $P < .05$ , ANOVA). CCH, carbachol; WT, wild type.

strongly Tmem16a dependent, as almost no ATP-induced secretion was observed in organoids of Tmem16a-knockout mice (Figure 4B and C, KO\_ATP.mp4). In contrast, CCH caused Paneth cell secretion even in the absence of Tmem16a, although the release was somewhat delayed (Figure 4B and C, KO\_CCH.mp4). These results establish a novel regulation of apical exocytosis of granules in Paneth cells Tmem16a/f.

### Differential Requirement of Tmem16a and Tmem16f for ATP- and CCH-Induced Release of Granules

We further examined how granular release by ATP and CCH depend on both Tmem16a and Tmem16f. In the absence of Tmem16a, ATP-induced release was strongly attenuated, whereas knockout of Tmem16f did not affect Paneth cell secretion (Figure 5A and B). These results correspond to the primarily apical expression of purinergic receptors<sup>28,29</sup> and the apical localization to Tmem16a (Figure 1A). In contrast, muscarinic M3 receptors and Tmem16f are both located at the basolateral pole of Paneth cells<sup>30</sup> (Figure 1A). Granular release induced by muscarinic stimulation (CCH) was hardly affected by knockout of apically located Tmem16a but was significantly reduced in the absence of Tmem16f (Figure 5C). Notably, niclosamide, a potent inhibitor of both Tmem16a and Tmem16f,<sup>20,31</sup> additionally inhibited granular release by ATP or CCH in Paneth cell lacking Tmem16f. The results demonstrate the importance of both Tmem16a and Tmem16f for fusion of granules in Paneth cells and release of their content into the crypt lumen.

### Attenuated Ca<sup>2+</sup> Signaling in Intestinal Epithelial Cells From Tmem16a<sup>-/-</sup> and Tmem16f<sup>-/-</sup> Mice

Previous studies indicated a role of Tmem16 proteins for intracellular Ca<sup>2+</sup> signaling in intestinal enterocytes and intestinal goblet cells.<sup>20,27</sup> We therefore examined the role of Tmem16a and Tmem16f for intracellular Ca<sup>2+</sup> signaling in Paneth cells when elicited by stimulation of with ATP or CCH. Stimulation of purinergic receptors with ATP or muscarinic receptors with CCH induced a typical peak/plateau Ca<sup>2+</sup> increase, which is due to Ca<sup>2+</sup> release from the ER Ca<sup>2+</sup> store (peak) and Ca<sup>2+</sup> influx through store-operated Ca<sup>2+</sup> entry channels (Figure 6A and C-F). Basal Ca<sup>2+</sup> was found to be lower in Paneth cells from Tmem16a<sup>-/-</sup> mice (Figure 6A and B). ATP-induced Ca<sup>2+</sup> peak and plateau were significantly reduced in cells from both Tmem16a<sup>-/-</sup> and Tmem16f<sup>-/-</sup> mice (Figure 6C and D). CCH-induced Ca<sup>2+</sup> peak and plateau were only reduced in Paneth cells from Tmem16a<sup>-/-</sup> mice. The data demonstrate the impact of Tmem16a/f on secretory intracellular Ca<sup>2+</sup> signals that are relevant for fusion of granules with the luminal membrane and release of their content.

### Enhanced Bacterial Content and Attenuated Programmed Cell Death in Jejunum and Ileum of Tmem16a<sup>-/-</sup> and Tmem16f<sup>-/-</sup> Mice

Granules of Paneth cells contain antimicrobial peptides, cytokines, and other factors that control proliferation or epithelial cell death.<sup>3,5,32,33</sup> We therefore analyzed the presence of Gram-positive and Gram-negative bacteria in jejunum and ileum of WT, Tmem16a<sup>-/-</sup>, and Tmem16f<sup>-/-</sup> mice. The number of bacteria was enhanced in the ileum of

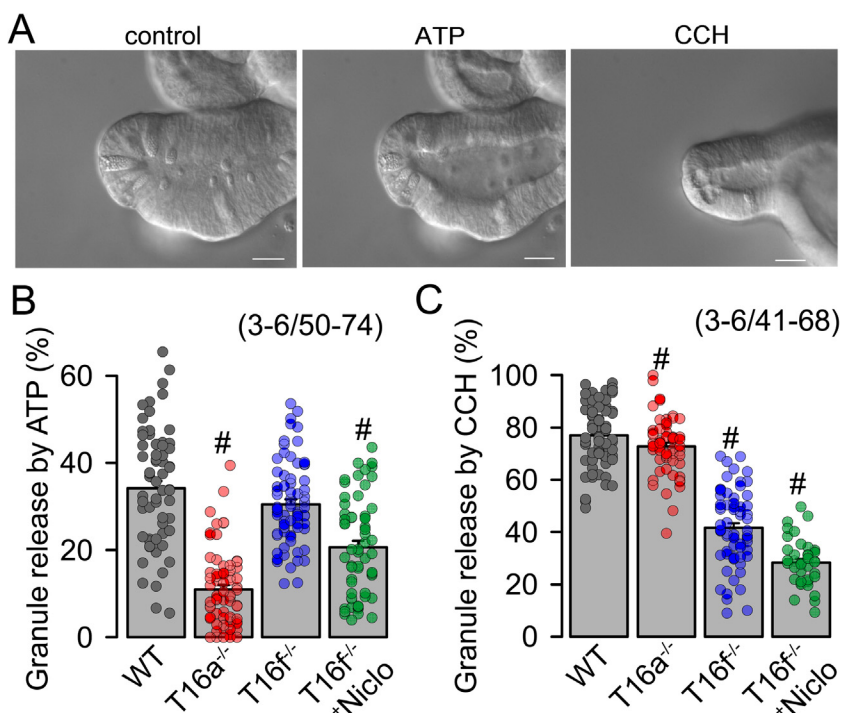


**Figure 5.** ATP- and CCH-induced release of granules from Paneth cells is inhibited in Tmem16a<sup>-/-</sup> and Tmem16f<sup>-/-</sup> organoids and in the presence of niclosamide. (A) ATP (100  $\mu$ M) and CCH (10  $\mu$ M) induced release of granules from Paneth cells in WT jejunal organoids. Bars = 20  $\mu$ m. (B) Percent of granules being release by stimulation with ATP in WT, T16a<sup>-/-</sup> and T16f<sup>-/-</sup> organoids, and in WT organoids in the presence of the Tmem16a/b blocker niclosamide (Niclo; 5  $\mu$ M). (C) Percent of granules being release by stimulation with CCH in WT, T16a<sup>-/-</sup> and T16f<sup>-/-</sup> organoids, and in WT organoids in the presence of niclosamide. Bars = 20  $\mu$ m. Mean  $\pm$  standard error of the mean (number of animals and cells analyzed). #significant difference from WT and T16f<sup>-/-</sup>, respectively ( $P < .05$ , analysis of variance). CCH, carbachol; WT, wild type.

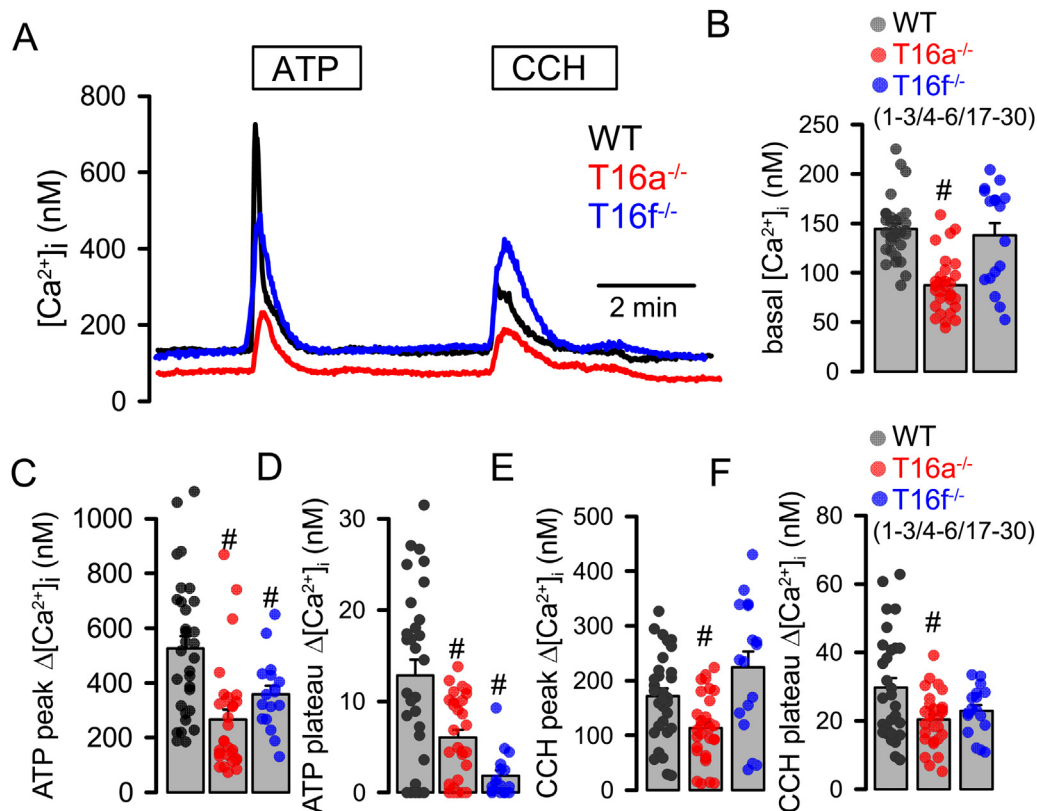


**Figure 6.** Attenuated  $Ca^{2+}$  signaling in intestinal epithelial cells from *Tmem16a*<sup>-/-</sup> and *Tmem16f*<sup>-/-</sup> mice. (A) Original recording of the intracellular  $Ca^{2+}$  concentration in Paneth cells from *Tmem16a*<sup>+/+</sup>, *Tmem16a*<sup>-/-</sup>, and *Tmem16f*<sup>-/-</sup> mice and the effects of ATP (100  $\mu$ M) and CCH (100  $\mu$ M). (B) Basal intracellular  $Ca^{2+}$  concentrations in Paneth cells from *Tmem16a*<sup>+/+</sup>, *Tmem16a*<sup>-/-</sup>, and *Tmem16f*<sup>-/-</sup> mice. (C–F) ATP and CCH induced increase in intracellular  $Ca^{2+}$  (peak and plateau) in Paneth cells from *Tmem16a*<sup>+/+</sup>, *Tmem16a*<sup>-/-</sup>, and *Tmem16f*<sup>-/-</sup> mice. Mean  $\pm$  standard error of the mean (number of animals/numbers of organoids/number of cells). #significant difference from WT ( $P < .05$ , analysis of variance). CCH, carbachol; WT, wild type.

*Tmem16a*<sup>-/-</sup> and *Tmem16f*<sup>-/-</sup> mice and in the jejunum of *Tmem16f*<sup>-/-</sup> mice, suggesting a reduced antimicrobial activity in the absence of *Tmem16* proteins (Figure 7). We also compared regulated cell death of intestinal epithelial cells in jejunum of WT and *Tmem16* knockout animals. Using TUNEL assays, we found a largely reduced number of cell death in both *Tmem16a*<sup>-/-</sup> and *Tmem16f*<sup>-/-</sup> mice. Taken together, the present results unmasked a crucial role of *Tmem16a* and *Tmem16f* for Paneth cell secretion. *Tmem16a/f* maintains secretory intracellular  $Ca^{2+}$  signals highly relevant for exocytosis of granules and proper Paneth cell function. A diversity of small molecules and natural compounds exist that either activate or inhibit *Tmem16a* and *Tmem16f*.<sup>21,34,35</sup> The present findings may therefore provide the basis for a novel anti-inflammatory therapy for intestinal diseases and may improve our understanding of the molecular mechanism of some of the currently available drugs.<sup>36–38</sup>

## Discussion

### Exocytosis is Controlled by *Tmem16a* and *Tmem16f*

Paneth cells are abundant in the crypt base of small intestine and are occasionally found in the proximal colon. A

series of studies have elucidated secreted products that are released by Paneth cells. The most well-known granule contents are the antimicrobial peptides such as lysozyme and  $\alpha$ -defensins, phospholipase A2, cytokines (interleukin 17A and tumor necrosis factor- $\alpha$ ) and proteases such as metalloproteinase 7.<sup>1</sup> Granules are exocytosed on contact to luminal LPS, which is a relatively slow process, suggesting a constitutive fusion of single granules with the apical membrane.<sup>4</sup> Paneth cells do not express TLR4, the receptor for LPS.<sup>10–12</sup> However, LPS can induce ATP release,<sup>15</sup> and we therefore propose that LPS-induced ATP release triggers regulated (sometimes called constitutive) exocytosis by increasing  $Ca^{2+}$  in the apical Paneth cell compartment.<sup>39</sup> In contrast, sudden massive compound exocytosis can be triggered by stimulation of basolateral M3 receptors similar to compound exocytosis of mucus in goblet cells.<sup>39</sup> Compound exocytosis is characterized by prefusion of granules, which provides a mechanism where deeper lying granules can readily release their content without having to be transported to the apical cell membrane.<sup>39,40</sup> The present study shows that both *Tmem16a* and *Tmem16f* are required for proper exocytosis. We propose that ATP could induce the release of exocytic granules from Paneth cells or goblet cells<sup>18</sup> via so-called regulated exocytosis,<sup>18</sup> which requires

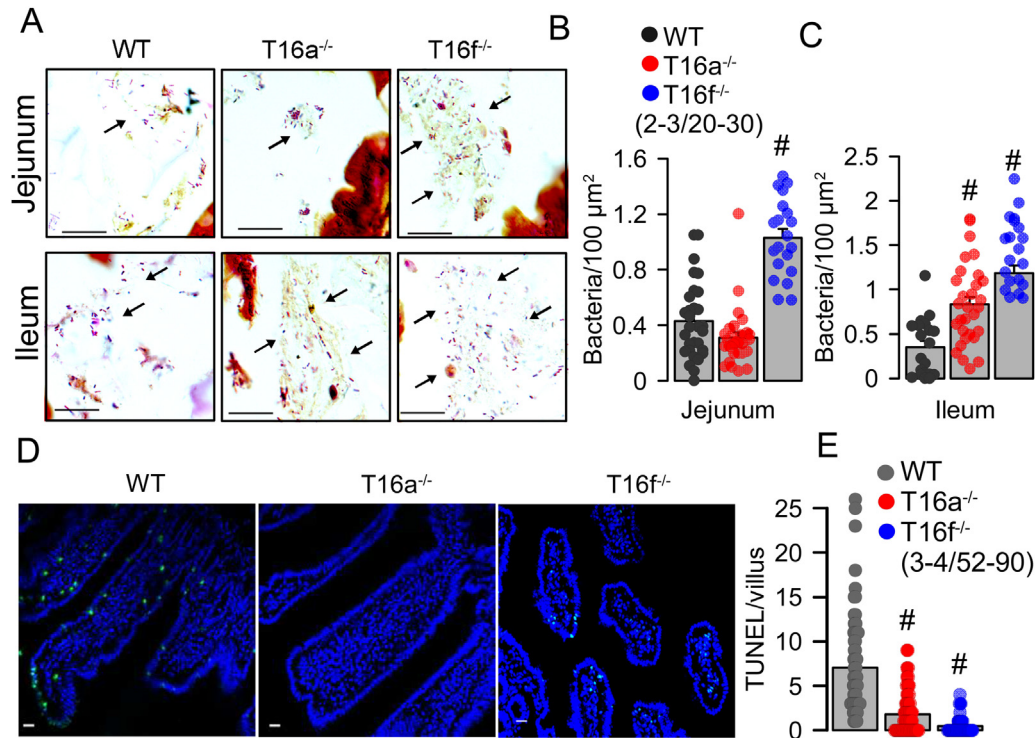


**Figure 7.** Enhanced bacterial content and attenuated programmed cell death in jejunum and ileum of *Tmem16a*<sup>-/-</sup> and *Tmem16f*<sup>-/-</sup> mice. (A) Gram-positive and Gram-negative bacteria in jejunum and ileum of WT, *T16a*<sup>-/-</sup>, and *T16f*<sup>-/-</sup> mice. Bars = 20 μm. (B, C) Numbers of bacteria in jejunum and ileum of WT, *T16a*<sup>-/-</sup>, and *T16f*<sup>-/-</sup> mice. Mean ± standard error of the mean (number of animals and villi analyzed). #significant difference from WT ( $P < .05$ , Kruskal-Wallis Test; H-Test). (D) TUNEL signals detected in jejunum of WT, *T16a*<sup>-/-</sup>, and *T16f*<sup>-/-</sup> mice. Bars = 20 μm. (E) Number of TUNEL positive cells per villus in jejunum of WT, *T16a*<sup>-/-</sup>, and *T16f*<sup>-/-</sup> mice. Mean ± standard error of the mean (number of animals and jejunal sections analyzed). #significant difference from WT ( $P < .05$ , analysis of variance). WT, wild type.

apical TMEM16A (c.f. Videos WT\_ATP.mp4 and KO\_ATP.mp4). TMEM16A is inhibited by Ani9 and by AO1, which also inhibits regulated exocytosis. In contrast, CCH possibly induces the release of Paneth cell granules by compound exocytosis, which requires the function of basolateral TMEM16F<sup>18</sup> (c.f. Videos WT\_CCH.mp4 and KO\_CCH.mp4). In contrast to TMEM16A, TMEM16F is not inhibited by AO1 or Ani9. AO1 and Ani9 inhibited not only TMEM16A and regulated exocytosis but also inhibited ATP-induced Ca<sup>2+</sup> signaling.<sup>16,18,41</sup> Taken together, *Tmem16a*, being located in the apical membrane, appears to be more relevant for regulated exocytosis, whereas *Tmem16f* located at the basolateral pole could be important for compound exocytosis.

### Intracellular Ca<sup>2+</sup> Signals are Shaped by *Tmem16* Proteins

Both *Tmem16a* and *Tmem16f* may control mucus release in intestinal and airway goblet cells by different mechanisms.<sup>18,20,23</sup> In large intestine, we and others found expression of TMEM16A predominantly, but not exclusively, in basolateral (particularly lateral) membranes of colonic crypt cells.<sup>18,27,42</sup> It was shown that *Tmem16a* tethers

the ER to the apical membrane. This leads to efficient receptor-mediated Ca<sup>2+</sup> store release and Ca<sup>2+</sup>-dependent fusion of vesicles/granules with the apical membrane.<sup>16,17,43,44</sup> In contrast, *Tmem16f* is a phospholipid scramblase and an ion channel and could have 2 functions: It might promote membrane fusion to form giant granules, which are known to be formed during compound exocytosis. For example, membrane fusion by *Tmem16f* was also observed for SARS-CoV-2-induced syncytia formation.<sup>45-47</sup> However, *Tmem16f* also allows permeation of Ca<sup>2+</sup> and may thereby support ATP-induced increase in intracellular Ca<sup>2+</sup> as shown in the present study and in previous studies.<sup>48</sup>

### Consequences of Loss of Function of *Tmem16a* and *Tmem16f*: Possible Therapeutic Targets in Intestinal Disease

*Tmem16a* is expressed in numerous tissues, preferentially in epithelial cells. Thus, a loss of function has numerous consequences, including compromised exocytosis, lower expression of proteins in the plasma membrane, and attenuated secretion of mucus and electrolytes.<sup>18,20,23,49</sup> In contrast, *Tmem16f* is highly expressed in macrophages, B-lymphocytes, platelets, and osteoblasts, and therefore,



loss of function causes immune defense, hemostasis, and bone mineralization.<sup>50–52</sup>

In our intestinal epithelial-specific *Tmem16a/f* knockout mice, we found an enhanced bacterial content in the intestine, which is related to the attenuated Paneth cell exocytosis and lower release of antimicrobial compounds (Figure 7). We also detected a reduced rate of apoptosis/necroptosis.<sup>33</sup> Notably, Paneth cells also express and release trophic factors, such as epidermal growth factor and mediators of the Wnt and Notch signaling pathway. These factors regulate intestinal stem cell homeostasis, secretory cell differentiation, and death of aged cells.<sup>3,32,33</sup> In this context, it is interesting to note that TMEM16F is required for activation of the metalloproteinases ADAM10 and ADAM17.<sup>53,54</sup> ADAM10 is expressed throughout the intestinal epithelium where it induces shedding of epithelial growth hormone receptors.<sup>55</sup>

Intestinal inflammatory diseases such as Crohn's disease, necrotizing enterocolitis, and intestinal microbiota dysbiosis have been related to abnormal Paneth cell physiology.<sup>5,56</sup> Along this line, we reported the first 2 patients with a loss-of-function mutation in TMEM16A, which suffered from recurrent episodes of hemorrhagic diarrhea and necrotizing enterocolitis.<sup>57</sup> Meanwhile, many small molecules and numerous natural or herbal compounds have been identified that either inhibit or activate *Tmem16a* and *Tmem16f*.<sup>21,22,31,34,37,58,59</sup> Some of these compounds may turn out to be useful therapeutics in inflammatory bowel disease, intestinal allergies, or abnormal colonization of the gut. Activators of TMEM16A such as the compound ETX001/ETD001 are currently under evaluation for the treatment of cystic fibrosis (CF; <https://www.clinicaltrials.gov/>). It is assumed to restore an apical Cl<sup>-</sup> conductance in airways of CF patients, which lack functional cystic fibrosis conductance regulator Cl<sup>-</sup> channels. Our team, however, does not support the use of TMEM16A activators in CF airways, as we have shown that activation of TMEM16A leads to an increase in mucus production and mucus secretion<sup>20,21</sup> and present study. However, activation of TMEM16A and consecutive release from Paneth cells and secretion of protective intestinal mucus might be well beneficial to patients suffering from various forms of inflammatory bowel disease.

## Study Approval

All animal experiments complied with the ARRIVE guidelines and were carried out in accordance with the UK Animals (Scientific Procedures) Act 1986 and associated guidelines, as well as EU Directive 2010/63/EU for animal experiments. The study was approved by the local Ethics Committee of the Government of Unterfranken (RUF-55.2.2-2532-2-677-19; approved on August 24, 2018), and our investigations were carried out in accordance with the Guide for the Care and authorities at the University of Kiel (project agreement no #1130).

## Supplementary Materials

Material associated with this article can be found in the online version at <https://doi.org/10.1016/j.gastha.2022.08.002>.

## References

1. Bevins CL, Salzman NH. Paneth cells, antimicrobial peptides and maintenance of intestinal homeostasis. *Nat Rev Microbiol* 2011;9:356–368.
2. Cray P, Sheahan BJ, Dekaney CM. Secretory Sorcery: paneth cell control of intestinal repair and homeostasis. *Cell Mol Gastroenterol Hepatol* 2021;12:1239–1250.
3. Ouellette AJ. Paneth cells and innate immunity in the crypt microenvironment. *Gastroenterology* 1997;113:1779–1784.
4. Yokoi Y, Nakamura K, Yoneda T, et al. Paneth cell granule dynamics on secretory responses to bacterial stimuli in enteroids. *Sci Rep* 2019;9:2710.
5. Riba A, Olier M, Lacroix-Lamadé S, et al. Paneth cell defects induce microbiota dysbiosis in mice and promote visceral hypersensitivity. *Gastroenterology* 2017;153:1594–1606.e2.
6. Farin HF, Karthaus WR, Kujala P, et al. Paneth cell extrusion and release of antimicrobial products is directly controlled by immune cell-derived IFN-gamma. *J Exp Med* 2014;211:1393–1405.
7. King SL, Mohiuddin JJ, Dekaney CM. Paneth cells expand from newly created and preexisting cells during repair after doxorubicin-induced damage. *Am J Physiol Gastrointest Liver Physiol* 2013;305:G151–G162.
8. Fernandez-Cabezudo MJ, Lorke DE, Azimullah S, et al. Cholinergic stimulation of the immune system protects against lethal infection by *Salmonella enterica* serovar Typhimurium. *Immunology* 2010;130:388–398.
9. Darby M, Schnoeller C, Vira A, et al. The M3 muscarinic receptor is required for optimal adaptive immunity to helminth and bacterial infection. *Plos Pathog* 2015;11:e1004636.
10. Tanabe H, Ayabe T, Bainbridge B, et al. Mouse paneth cell secretory responses to cell surface glycolipids of virulent and attenuated pathogenic bacteria. *Infect Immun* 2005;73:2312–2320.
11. Price AE, Shamardani K, Lugo KA, et al. A map of toll-like receptor expression in the intestinal epithelium reveals distinct spatial, cell type-specific, and temporal patterns. *Immunity* 2018;49:560–575.e6.
12. Lorenz E, Patel DD, Hartung T, et al. Toll-like receptor 4 (TLR4)-deficient murine macrophage cell line as an in vitro assay system to show TLR4-independent signaling of *Bacteroides fragilis* lipopolysaccharide. *Infect Immun* 2002;70:4892–4896.
13. Kopp F, Kupsch S, Schromm AB. Lipopolysaccharide-binding protein is bound and internalized by host cells and colocalizes with LPS in the cytoplasm: implications for a role of LBP in intracellular LPS-signaling. *Biochim Biophys Acta* 2016;1863:660–672.
14. Hansen GH, Rasmussen K, Niels-Christiansen LL, et al. Lipopolysaccharide-binding protein: localization in secretory granules of paneth cells in the mouse small intestine. *Histochem Cell Biol* 2009;131:727–732.

15. Silberfeld A, Chavez B, Obidike C, et al. LPS-mediated release of ATP from urothelial cells occurs by lysosomal exocytosis. *Neurourol Urodyn* 2020;39:1321–1329.
16. Cabrita I, Benedetto R, Fonseca A, et al. Differential effects of anoctamins on intracellular calcium signals. *FASEB J* 2017;31:2123–2134.
17. Jin X, Shah S, Liu Y, et al. Activation of the Cl<sup>-</sup> channel ANO1 by localized calcium signals in nociceptive sensory neurons requires coupling with the IP3 receptor. *Sci Signal* 2013;6:ra73.
18. Benedetto R, Cabrita I, Schreiber R, et al. TMEM16A is indispensable for basal mucus secretion in airways and intestine. *FASEB J* 2019;33:4502–4512.
19. Cabrita I, Benedetto R, Wanitchakool P, et al. TMEM16A mediated mucus production in human airway epithelial cells. *Am J Respir Cell Mol Biol* 2021;64:50–58.
20. Cabrita I, Benedetto R, Schreiber R, et al. Niclosamide repurposed for the treatment of inflammatory airway disease. *JCI Insight* 2019;8:128414.
21. Kunzelmann K, Ousingsawat J, Cabrita I, et al. TMEM16A in cystic fibrosis: activating or inhibiting? *Front Pharmacol* 2019;10:3.
22. Cheng Y, Feng S, Puchades C, et al. Identification of a conserved drug binding pocket in TMEM16 proteins. *Res Sq* 2022;rs.3.rs-1296933.
23. Benedetto R, Ousingsawat J, Wanitchakool P, et al. Epithelial chloride transport by CFTR requires TMEM16A. *Scientific Rep* 2017;7:12397.
24. Mahe MM, Aihara E, Schumacher MA, et al. Establishment of gastrointestinal epithelial organoids. *Curr Protoc Mouse Biol* 2013;3:217–240.
25. Altay G, Battle E, Fernández-Majada V, et al. In vitro Self-organized mouse small intestinal epithelial monolayer protocol. *Bio Protoc* 2020;10:e3514.
26. Schneider CA, Rasband WS, Eliceiri KW. NIH Image to ImageJ: 25 years of image analysis. *Nat Methods* 2012;9:671–675.
27. Schreiber R, Faria D, Skryabin BV, et al. Anoctamins support calcium-dependent chloride secretion by facilitating calcium signaling in adult mouse intestine. *Pflügers Arch* 2015;467:1203–1213.
28. Robaye B, Ghanem E, Wilkin F, et al. Loss of nucleotide regulation of epithelial chloride transport in the jejunum of P2Y4-null mice. *Mol Pharmacol* 2003;63:777–783.
29. Ghanem E, Robaye B, Leal T, et al. The role of epithelial P2Y2 and P2Y4 receptors in the regulation of intestinal chloride secretion. *Br J Pharmacol* 2005;146:364–369.
30. McLean LP, Smith A, Cheung L, et al. Type 3 muscarinic receptors contribute to intestinal mucosal homeostasis and clearance of *nippostrongylus brasiliensis* through induction of TH2 cytokines. *Am J Physiol Gastrointest Liver Physiol* 2016;311:G130–G141.
31. Miner K, Labitzke K, Liu B, et al. Drug repurposing: the Anthelmintics niclosamide and Nitazoxanide are potent TMEM16A Antagonists that fully Bronchodilate airways. *Front Pharmacol* 2019;10:51.
32. Hirao LA, Grishina I, Bourry O, et al. Early mucosal sensing of SIV infection by paneth cells induces IL-1 $\beta$  production and initiates gut epithelial disruption. *Plos Pathog* 2014;10:e1004311.
33. Günther C, Neumann H, Neurath MF, et al. Apoptosis, necrosis and necroptosis: cell death regulation in the intestinal epithelium. *Gut* 2013;62:1062–1071.
34. Namkung W, Yao Z, Finkbeiner WE, et al. Small-molecule activators of TMEM16A, a calcium-activated chloride channel, stimulate epithelial chloride secretion and intestinal contraction. *FASEB J* 2011;25:4048–4062.
35. Tradtrantip L, Ko EA, Verkman AS. Antidiarrheal efficacy and cellular mechanisms of a Thai herbal remedy. *PLoS Negl Trop Dis* 2014;8:e2674.
36. Tradtrantip L, Namkung W, Verkman AS. Crofelemer, an antisecretory antidiarrheal proanthocyanidin oligomer extracted from croton lechleri, targets two distinct intestinal chloride channels. *Mol Pharmacol* 2010;77:69–78.
37. Namkung W, Thiagarajah JR, Phuan PW, et al. Inhibition of Ca<sup>2+</sup>-activated Cl<sup>-</sup> channels by gallotannins as a possible molecular basis for health benefits of red wine and green tea. *FASEB J* 2010;24:4178–4186.
38. Kitabatake M, Matsumura Y, Ouji-Sageshima N, et al. Persimmon-derived tannin ameliorates the pathogenesis of ulcerative colitis in a murine model through inhibition of the inflammatory response and alteration of microbiota. *Sci Rep* 2021;11:7286.
39. Pickett JA, Edwardson JM. Compound exocytosis: mechanisms and functional significance. *Traffic* 2006;7:109–116.
40. Thorn P, Gaisano H. Molecular control of compound exocytosis: a key role for VAMP8. *Commun Integr Biol* 2012;5:61–63.
41. Centeio R, Cabrita I, Benedetto R, et al. Pharmacological inhibition and activation of the Ca(2+) activated Cl(-) channel TMEM16A. *Int J Mol Sci* 2020;21:2557.
42. He Q, Halm ST, Zhang J, et al. Activation of the basolateral membrane Cl conductance essential for electrogenic K secretion suppresses electrogenic Cl secretion. *Exp Physiol* 2011;96:305–316.
43. Jin X, Shah S, Du X, et al. Activation of Ca<sup>2+</sup>-activated Cl<sup>-</sup> channel ANO1 by localized Ca<sup>2+</sup> signals. *J Physiol* 2016;594:19–30.
44. Kunzelmann K, Cabrita I, Wanitchakool P, et al. Modulating Ca<sup>2+</sup> signals: a common theme for TMEM16, Ist2, and TMC. *Pflügers Arch* 2016;468:475–490.
45. Suzuki J, Umeda M, Sims PJ, et al. Calcium-dependent phospholipid scrambling by TMEM16F. *Nature* 2010;468:834–838.
46. Deisl C, Hilgemann DW, Syeda R, et al. TMEM16F and dynamins control expansive plasma membrane reservoirs. *Nat Commun* 2021;12:4990.
47. Braga L, Ali H, Secco I, et al. Drugs that inhibit TMEM16 proteins block SARS-CoV-2 Spike-induced syncytia. *Nature* 2021;594:88–93.
48. Yang H, Kim A, David T, et al. TMEM16F forms a Ca(2+)-activated cation channel required for lipid scrambling in platelets during blood coagulation. *Cell* 2012;151:111–122.
49. Benedetto R, Ousingsawat J, Cabrita I, et al. Plasma membrane localized TMEM16 proteins are indispensable for expression of CFTR. *J Mol Med (Berl)* 2019;97:711–722.

50. Ousingsawat J, Wanitchakool P, Kmit A, et al. Anoctamin 6 mediates effects essential for innate immunity downstream of P2X7-receptors in macrophages. *Nat Commun* 2015;6:6245.
51. Mattheij NJ, Braun A, van Kruchten R, et al. Survival protein anoctamin-6 controls multiple platelet responses including phospholipid scrambling, swelling, and protein cleavage. *FASEB J* 2015;30:727–737.
52. Ehlen HW, Chinenkova M, Moser M, et al. Inactivation of Anoctamin-6/Tmem16f, a regulator of phosphatidylserine scrambling in osteoblasts, leads to decreased mineral deposition in skeletal tissues. *J Bone Miner Res* 2012;28:246–259.
53. Sommer A, Kordowski F, Buch J, et al. Phosphatidylserine exposure is required for ADAM17 sheddase function. *Nat Commun* 2016;7:11523.
54. Bleibaum F, Sommer A, Veit M, et al. ADAM10 sheddase activation is controlled by cell membrane asymmetry. *J Mol Cell Biol* 2019;11:979–993.
55. Dempsey PJ. Role of ADAM10 in intestinal crypt homeostasis and tumorigenesis. *Biochim Biophys Acta Mol Cell Res* 2017;1864:2228–2239.
56. Gassler N. Paneth cells in intestinal physiology and pathophysiology. *World J Gastrointest Pathophysiol* 2017;8:150–160.
57. Park JH, Ousingsawat J, Cabrera I, et al. TMEM16A deficiency: a potentially fatal neonatal disease resulting from impaired chloride currents. *J Med Genet* 2020; 58:247–253.
58. Zhong J, Xuan W, Tang M, et al. Advances in anoctamin 1: a potential new drug target in medicinal chemistry. *Curr Top Med Chem* 2021;21:1139–1155.
59. Wang T, Wang H, Yang F, et al. Honokiol inhibits proliferation of colorectal cancer cells by targeting anoctamin 1/TMEM16A Ca<sup>2+</sup>-activated Cl<sup>-</sup> channels. *Br J Pharmacol* 2021;178:4137–4154.

---

Received May 10, 2022. Accepted August 3, 2022.

**Correspondence:**

Address correspondence to: Karl Kunzelmann, MD, University of Regensburg, Physiology, University street 31, Regensburg, Germany 93053. e-mail: [karl.kunzelmann@ur.de](mailto:karl.kunzelmann@ur.de).

**Acknowledgments:**

The technical assistance by Patricia Seeberger is greatly appreciated.

**Authors' Contributions:**

Rainer Schreiber, Ines Cabrera, and Karl Kunzelmann contributed to conceptualization, methodology, validation, writing, reviewing, and editing the article. Rainer Schreiber and Ines Cabrera contributed to formal analysis and investigation. Rainer Schreiber and Karl Kunzelmann contributed to funding acquisition. All authors have read and agreed to the published version of the manuscript.

**Conflicts of Interest:**

The authors disclose no conflicts.

**Funding:**

This study was supported by DFG KU756/14-1, DFG project number 387509280, SFB 1350 (project A3).

**Ethical Statement:**

The corresponding author, on behalf of all authors, jointly and severally, certifies that their institution has approved the protocol for any investigation involving humans or animals and that all experimentation was conducted in conformity with ethical and humane principles of research.

**Data Transparency Statement:**

All data, analytic methods, and study materials will be made available to other researchers on request. Please contact directly Prof. Dr Rainer Schreiber ([rainer.schreiber@ur.de](mailto:rainer.schreiber@ur.de)).